Spring 2017

Using computational tools to design a molecularly imprinted polymer with selectivity and high affinity for acetylcholine

Nathaniel Donald Thiemann
Trinity College, Hartford Connecticut, nathaniel.thiemann@trincoll.edu

TRINITY COLLEGE

USING COMPUTATIONAL TOOLS TO DESIGN A MOLECULARLY IMPRINTED POLYMER WITH SELECTIVITY AND HIGH AFFINITY FOR ACETYLCHOLINE

BY

Nathaniel Thiemann

A THESIS SUBMITTED TO THE FACULTY OF THE NEUROSCIENCE PROGRAM IN CANDIDACY FOR THE BACCALAUREATE DEGREE WITH HONORS IN NEUROSCIENCE

NEUROSCIENCE PROGRAM

HARTFORD, CONNECTICUT

May 6, 2017

USING COMPUTATIONAL TOOLS TO DESIGN A MOLECULARLY IMPRINTED POLYMER WITH SELECTIVITY AND HIGH AFFINITY FOR ACETYLCHOLINE

BY

Nathaniel Thiemann

Honors Thesis Committee

Approved:

_____

Vindya Thilakarathne, Thesis Advisor

_____

William Church, Thesis Committee

_____

Charles Swart, Thesis Committee

_____

Sarah Raskin, Director, Neuroscience Program

Date: _____

Abstract:

Nanomaterials are artificial materials that have been engineered to have special chemical properties. Molecularly imprinted polymers are a type of nanomaterial, which contain recognition sites with high selectivity and affinity for a template element. A neuroethological and computational approach was taken to rationally design a molecularly imprinted polymer for the neurotransmitter acetylcholine. The program AutoDock was used to study interactions of acetylcholine with the protein acetylcholinesterase. It was found acetylcholine interacts with the protein through hydrogen bonding, ionic interactions, and pi-cation interactions. The results of the docking study were used to select five functional monomers that could potentially engage in similar non-covalent interactions with acetylcholine. Density functional theory calculations were then performed with the General Atomic and Molecular Electronic Structure System to determine what functional monomer in complex with acetylcholine had the lowest stabilization energy. Results indicated that itaconic acid formed the most favorable complex with acetylcholine *in silico*. Therefore, itaconic acid is a promising candidate for future attempts to synthesize an acetylcholine molecularly imprinted polymer. Such a polymer could have applications in chromatography, biosensors, and biomedical devices. Of particular note, an acetylcholine molecularly imprinted polymer could be efficacious in developing a motor prosthesis with higher temporal and spatial resolution.

Significance Statement:

Other peer reviewed works have given precedent to the logic that chemicals that form low stabilization energy complexes with a template *in silico* are ideal candidates for implementation as functional monomers in a molecular imprinted polymer for that template. This computational method for identifying ideal functional monomer candidates is more economically and

environmentally friendly compared to alternatives such as the bulk polymerization method. In future, the results of this study can be used in an attempt to synthesize an acetylcholine molecularly imprinted polymer. Additionally, the results of any attempted synthesis could be used to cross-examine the validity of the results from this study. If validated, then this study will also further validate the *in silico* design of molecularly imprinted polymers. Furthermore, this study would provide evidence that template-functional monomer pairings can be optimized using free software and access to a modern computer.

Introduction:

Nanomaterials are artificial materials that have been manipulated at the nanoscale to have unique properties. Molecularly imprinted polymers (MIPs) are a type of nanomaterial, that possess properties ranging from embedded recognition elements to special phenotypic qualities (Algieri, 2014). MIPs made for element recognition have high specificity and affinity for their imprinted template. MIPs have been imprinted to templates ranging in size from single molecules to entire cells (Alexander, 2006) Although the materials and methodology used for their synthesis vary greatly, MIPs meant for template recognition typically feature several ubiquitous elements pre-polymerization: the template, functional monomer(s), solvent, cross-linking agent, and initiating agent. The template is the element for which the polymer is desired to have the capacity to recognize. Functional monomers are essentially the building blocks of the MIP, and form a complex with the template that will be cast into the recognition site. For this reason, functional monomers that can form reversible non-covalent interactions with the template are ideal. The porogenic solvent is a chemical that both the chosen template and functional monomer are both miscible in. Cross-linking agents are used to link together the template-functional monomer complexes into a single continuous polymer upon initiation. The initiating agent serves as a signal

that triggers the polymerization process. This signal can be the cross-linking agent itself, UV-radiation, or temperature change (Alexander, 2006).

Some specific purposes for which nanomaterials have been synthesized include: separation of molecules from various types of solutions (Ahmadi, 2011; Alexander, 2006; Khairi, 2015), drug delivery (Puoci, 2007), protein crystallization (Saridakis, 2011), scaffolding in tissue engineering (Suntornnond, 2016), imparting special phenotypic properties such as toughening (Askarinejad, 2015), signal recognition and transduction (Lattach, 2012), and providing an alternative method for antibody production (Nicholls, 2011). MIPs can be synthesized in many forms, although not all encompassing, the following list includes some archetypal MIPs of note: multi-layer membranes (De Luca, 2011), nanofilms (Jimenez-Solomon, 2016), sol-gels (Liu, 2016), hydrogels (Hadizadeh, 2013), and xerogels (Wach, 2013). These different types of MIPs are important, because they utilize different methods and types of environments in their syntheses. This allows greater versatility in terms of what chemicals scientists can utilize in their research, and the experimental conditions in which they can use to synthesize MIPs with different properties. For instance, Saridakis et al. synthesized hydrogels using the functional monomer acrylamide in water to synthesize a MIP that was functional in aqueous solution (Saridakis, 2011). Many types of MIP are unable to operate in aqueous solution, due to only being functional in organic solution, however utilizing hydrogels allowed this group to bypass this problem and develop a highly effective technique for protein isolation and eventual crystallization.

While the types of MIPs that can be synthesized are indeed numerous, the options for types of MIPs is dwarfed by their possible templates. In recent years there has been a flurry of peer reviewed works discussing MIPs synthesized for notable templates. Some notable biomolecules that MIPs have been synthesized to detect include: 17β-estradiol (Wei, 2007), benzylparaben

(Asman, 2015), bovine serum albumin (Liu, 2016), cholate salts (Yañez, 2010), cocaine (Piletska, 2005), diazinon (Bayat, 2014), fenitrothion (Barros, 2014), lactose (Hadizadeh, 2013), theophylline (Sun, 2006), MDMA (Ahmadi, 2011), tryptophan (Prasad and Rai, 2012), and urea (Chen, 2011). One extremely pertinent example of a reported MIP was made by Suedee et al. for the recognition of serotonin and dopamine. Suedee et al. synthesized an MIP with recognition sites selective for both the neurotransmitters, which they showed could be used to conduct competitive assays (Suedee, 2008). This unique example of a specialized assay for dopamine and serotonin highlights the unexplored potential for MIPs in the field of neuroscience.

Some lessons can be learned from these previous studies. First, it has been shown that it is best to use a crosslinking-agent to functional monomer ratio of 80%:20% (Algieri, 2014). Such a ratio typically ensures adequate mechanical stability and good recognition performance in the material yielded. It is also important for one to take into account the desired purpose (i.e. extraction, signal transduction, etc) and operational environment from the start when attempting to synthesize MIPs (Wei, 2006). Factors that have a major impact on these functions are the very chemicals used to make MIPs. This means that the solvent, template, functional monomer, cross-linking agent, and initiator that are chosen for use in polymerization must all be carefully chosen based upon what the desired function and application of the final product are. Additionally, the relative ratios of all the chemicals being used must be appropriate, to ensure adequate size and distribution of the imprinted recognition sites. It is also important that there are little to no side reactions between the chemicals used, as that would also negatively affect the formation of the polymer (Wei, 2006). For this reason, experiments typically only use one species of functional monomer in MIP synthesis. These are all critical factors to keep in mind when attempting to synthesize MIPs with a high selectivity. Until recently, the fastest method to optimize all these

factors was through bulk polymerization methods, which are very expensive, labor intensive, and wasteful of valuable resources.

Thankfully, new computational approaches have provided researchers with a more affordable and less wasteful way to optimize their synthesis of MIPs. These approaches allow for scientists to screen a library of chemicals for their suitability in a variety of roles in a much more cost-efficient manner. The use of computational methods saves resources and allows for the rational design of MIPs that is more efficient than bulk polymerization. Several groups have set the precedent that a template-functional monomer complex with the lowest binding energy complex *in silico* is also the optimal functional monomer when synthesizing MIPs *in situ (*Ahmadi, 2011; Pavel, 2006). It seems that -COOH and -CH_2OH functional groups often play a large role in the most favorable template-functional monomer complexes (Pavel, 2006). Due to their successful implementation and growing efficiency, the use of computational tools to design MIPs is growing at a fast pace.

Although computational tools have been used by pharmaceutical companies to develop new pharmacological agents for years, their adaptation to synthesis of MIPs is relatively new. Nevertheless, there is already a large assembly of peer reviewed material available where scientists have utilized computational approaches to detail the intermolecular interactions between a template and functional monomer (Barros, 2014; Diñeiro, 2006; De Luca, 2011; Nicholls, 2009). Some higher end computational chemistry software can even factor in possible solvents and cross-linking agents when optimizing the chemicals for use in synthesis of MIPs (Ahmadi, 2011). These software help scientists predict chemical phenomena involved in MIP synthesis at a molecular level, which provides more efficient strategies for MIP design. It is important to note that there is a significant amount of trade-off between the accuracy of a computational chemistry calculation

and the cost-efficiency of doing so. Or in other words, more accurate calculations are typically more expensive to run in terms of computational time (Wei, 2006).

Molecular dynamics is one computational chemistry strategy that is commonly to compute meaningful metrics for the synthesis of MIPs (i.e. equilibrium geometry, Snyder polarity index, dielectric constants). Molecular dynamic calculations utilize Newtonian functions to compute the potential energy of a molecular system. The potential energy of the system is described by a force field, which is a stepwise integration of the Newtonian laws of motion meant to predict atomic positions at the global potential energy minimum. Molecular dynamics can also be used to determine the optimum solvent for use in polymerization of MIPs (Nicholls, 2009). Since molecular dynamics utilize Newtonian functions they can suffer from accuracy, especially in systems where the Newtonian function ends up not being linear (Crouch, 1997). Since the plot of total energy for many compounds is not linear (consider how favorability alters as you rotate substituents about a bond), this causes Newtonian functions to have limited applicability in calculating how favorable conformations of a large complex are. This barrier can often be overcome with logic and more computational power, but that drastically reduces the benefit of increased efficiency that makes computational approaches appealing.

Ab initio computational methods are a solution to the problem of accuracy with molecular dynamics. When one says *ab initio*, that person is referring to performing a computation from the start, or with the Schroedinger equation. The Schroedinger equation is a differential equation that combines wave theory from Newtonian mechanics and particle theory from de Broglie's equation. Although the full Schroedinger equation is so complex that it cannot be solved for systems with more than one electron, mathematicians have provided multiple ways to solve a simplified version of it by using approximations. One particularly popular derivative of *ab initio* computational

approaches includes density functional theory. Density functional theory then applies the electron density of an entire system to solve a simplified version of the Schroedinger equation. Density functional theory is considered a derivative of *ab initio* calculations, because it solves an *ab initio* problem using semi-empirical parameters, rather than starting from scratch. A typical correlational function used in density function theory is the Beck 3 parameter Lee Yang Parr (B3LYP) correlation functional, which takes 3 parameters to input the semi-empirical data for the calculation of the electron density of a system. Even using semi-empirical values, approximations must be made to solve the Schroedinger equation for systems with more than one electron. These approximations include the Born-Oppenheimer, Hartree-Fock, and linear combination of atomic orbitals. The Born-Oppenheimer approximation assumes nuclear movement is zero, thus making the repulsion from nuclei constant. The Hartree-Fock approximation assumes that each electron in a system moves independently of one another, which allows the presence that each electron feels from other electrons to be simplified into one constant field. Finally, the linear combination of atomic orbitals sets the total wave function of an atom or molecule equal to the product of one electron wave functions, or in other words the wave function for hydrogen. With these approximations and an appropriate basis set, it is possible to perform a highly accurate approximation of the Schroedinger equation for large electron systems ranging between 50-100 atoms (Crouch, 1997). A basis set is used to determine what atomic orbitals to use in linear combination of atomic orbitals, and can greatly affect the results of a density functional theory calculation. Typically the smallest basis set that can be used with reliable results is the 6-31G* basis set (Crouch, 1997)

Since it is typically desired for nanomaterials to have biomimetic properties, it is fitting that they are often designed by studying their biological source of inspiration. For example, when

trying to design a material that aided in climbing up sheer vertical surfaces, researches looked at the tokay gecko's foot. It was observed that this lizard's foot was able to selectively cling to surfaces due to specialized "spatula-like" hairs on their feet (Hawkes, 2015). These hairs dramatically increased the van der Waals force of attraction between the lizard's foot and a surface. These dispersion forces were so strong, that they allowed the tokay gecko to cling to surfaces selectively. This insight into the mechanism that a gecko uses to cling to a wall eventually led to the production of an innovative nanomaterial, which allowed a 70kg individual to cling to a vertical glass wall (Hawkes, 2015). This example serves as a lesson for how bio-mimetic approaches could be utilized to design a biosensor for acetylcholine that could be used in various applications.

In a similar bio-mimetic fashion to one applied to recapitulate the clinginess of the gecko's foot, scientists typically observe ligand-protein interactions in order to determine what functional groups facilitate their interaction (Saridakis, 2011). With insight into what functionalities cause a biological ligand-protein interaction to be energetically favorable, it becomes easier to rationally design a specific type of nanomaterial, molecularly imprinted polymers. acetylcholinesterase has previously been immobilized in several biosensors (Simon, 2015; Guan, 2012), the immobilization of enzymes in biosensors is not economically viable for large scale implementation (Nakamura, 2003). To the authors knowledge, no attempt has been made to make an acetylcholine molecularly imprinted polymer with non-biological recognition elements. Furthermore, polymers made using immobilized acetylcholinesterase have been noted to be unstable. Therefore, such polymers have short term viability while requiring expensive techniques to isolate and immobilize the protein (Nakamura, 2003). MIPs are favorable to immobilization of proteins for the purpose of detection due to the use of cheap and alterable functional monomers. Furthermore, these functional monomers form a stable polymer with a crosslinking agent and imprinted template, while

immobilized proteins are often highly unstable. Therefore, MIPs are a cheaper and more stable option than protein immobilization for the synthesis of a material with recognition capabilities (Ahmadi, 2011).

Acetylcholine is a neurotransmitter that is synthesized in the cell soma by the enzyme choline acetyl transferase. Acetylcholine is released from intracellular vesicular storage in circuit transmission between neurons, and binds to extracellular receptors. There are two families of acetylcholine receptors: nicotinic and muscarinic. Both families of receptors are named for their respective acetylcholine agonists, and are pentameric protein complexes. However, nicotinic receptors function as ionic channels, whereas muscarinic receptors function as G-protein coupled receptors. When acetylcholine binds to a post-synaptic nicotinic receptor it induces fast onset, brief duration, excitatory potential. Acetylcholine activation of muscarinic receptors induces slow onset, prolonged duration, excitatory or inhibitory potentials in pre- and post-synaptic cells.

Nicotinic receptors are known to be found on the post-synaptic muscle cells of the neuromuscular junction. Activation of these receptors induces an influx of sodium cations, which depolarize the cell, and cause the cell to contract. Once acetylcholine unbinds from a receptor, it is then rapidly hydrolyzed by acetylcholinesterase. This hydrolysis is performed by a serine protease active site consisting of Ser^{200}, His^{440}, and Glu^{327} (Sussman, 1991). Sussman et al. also indicated binding of acetylcholine to acetylcholinesterase is further facilitated by hydrogen bonding with Gly^{118} and Gly^{119}. Ionic and pi-cation interactions were also deemed to play a role in acetylcholine binding to acetylcholinesterase (Sussman, 1991).

Therefore, in this study we sought to gain a better understanding of the binding pocket that acetylcholinesterase has for acetylcholine with the docking software AutoDock. Autodock makes several approximations in order to make calculations of free binding energy of a ligand-protein.

The software first restricts the flexibility of the ligand and protein being analyzed, then makes a grid out of the protein. AutoDock finally docks the ligand in any space where it can physically fit, and calculates the interatomic potential of the ligand-protein complex at that site. The most favorable sites were ranked both by lowest binding energy and number hydrogen bonds formed. The results of the acetylcholine-acetylcholinesterase docking study were visualized with Maestro in order to better understand the interactions that drive acetylcholine into the active site of the protein. Afterwards, a library of functional monomers was selected that could potentially complex with acetylcholine in similar fashion to the active site amino acid residues of acetylcholinesterase. The molecular editor, Avogadro, was used to prepare input files consisting of the Cartesian coordinates and computational parameters for each acetylcholine-functional monomer complex. Complexes ranging from 1 acetylcholine: 1 functional monomer to 1 acetylcholine: 3 functional monomers were created for every functional monomer of interest. The quantum calculator, General Atomic and Molecular Electronic Structure System (GAMESS), was used to calculate the equilibrium geometry of all the prepared acetylcholine-functional monomer complexes. GAMESS is a semi-empirical program, that can be used to run *ab initio* calculations with customizable parameters. For instance, GAMESS can be used to compute transition structures, reaction coordinates, vibrational frequencies, and electrostatic potential in three dimensions. GAMESS is also parallelized for use on multiprocessor computers, and was run using server time donated by the group ChemCompute. The results from density functional theory calculations performed by GAMESS were analyzed with the visualization software MacMolPlt, and used to determine the lowest stabilization energy of the screened acetylcholine-functional monomer complexes. MacMolPlt is designed for displaying the output of GAMESS calculations as animations, and can also be utilized to visualize electronic properties or interactions. The results of this study will be

compared to future empirical results to determine the validity of the density functional theory calculations.

Materials and Methods

Experimental Design

The results of Sussman et al. were validated by doing a docking study of an acetylcholinesterase crystal structure that was found on Protein Data Bank (PDB, PDB code: 1EEA). Once we analyzed the results of the docking study and confirmed they were dependable, we chose functional monomers that have noted use in synthesizing MIPs. PDB, pubchem, and peer reviewed articles were used to obtain lattice constants for each functional monomer and acetylcholine. These lattice constants were used to create input files of acetylcholine-functional monomer complexes with appropriate parameters to create a supercell. A quantum calculator was then used to run density functional theory calculations to see which complex of functional monomers with acetylcholine had the lowest stabilization energy. It is expected that the lowest energy complex will serve to make the best performing acetylcholine MIPs. The results of the density function theory calculations will be validated by a later experiment.

AutoDock Analysis

The program AutoDock (http://autodock.scripps.edu/, RRID:SCR_012746) was downloaded along with an crystal structure of *Electrophorus electricus* acetylcholinesterase with acetylcholine bound to it from PDB (http://www.rcsb.org/pdb/explore.do?structureId=1EEA, RRID:SCR_006555). A new file for the receptor and ligand were saved in the same directory. The protein had all the water molecules in the structure removed and hydrogens added wherever needed. A grid of the protein was made and AutoDock was run via the command prompt in order

to dock acetylcholine in all the possible sites it could bind to the protein. The results were saved in the same directory as the accompanying intermediate files. The results of the docking study were analyzed with the visualization software PyMOL (https://www.pymol.org/, RRID:SCR_000305). The site with the most favorable binding energy was further analyzed with the program Maestro (https://www.schrodinger.com/maestro). This analysis was done so that the chemical interactions between acetylcholine and involved amino acid residues could be determined and cleanly visualized.

GAMESS Analysis

The quantum chemistry calculator GAMESS (http://www.msg.ameslab.gov/gamess/, RRID:SCR_014896) was used in order to calculate the equilibrium geometry, or lowest stabilization energy, for each acetylcholine-functional monomer complex. The program Avogadro (https://avogadro.cc/) was used to prepare the input files for GAMESS analysis. To prepare the input files, the structure for acetylcholine was retrieved from the crystal structure for acetylcholinesterase previously used in the AutoDock analysis. The crystal structures for the functional monomers methacrylic acid, acrylic acid, methacrylamide, and acrylamide were retrieved from Pubchem (https://pubchem.ncbi.nlm.nih.gov/, RRID:SCR_004742). The crystal structure for another functional monomer, itaconic acid, was replicated from the data provided by Graham et al. in 1997.

In each GAMESS input file, a copy of the acetylcholine crystal structure was in a complex with one to three functional monomer(s). The complex was put into a unit cell, which was organized so that the edges of the cell were always ~10Å away from the nearest Cartesian coordinate of an element within it. Before saving the parameters for the file, the complexes were relaxed via energy optimization with the MMFF94s force field (4 steps per update, steepest

descent, fixed/ignored atoms were movable) for 10-15 seconds to ensure the molecules were in a somewhat favorable confirmation. Afterwards, the files were saved as GAMESS input files meant to calculate the equilibrium geometry of the complex with the following parameters: Cartesian coordinates, B3LYP correlational functional, 6-31G(d,p) basis set, in gas phase. Density functional theory calculations for each complex were performed three times to ensure results. The energies for the template (acetylcholine) and each functional monomer were also calculated using density functional theory. A total of three calculations was also performed for each individual molecule (i.e. acetylcholine and each functional monomer being screened).

The GAMESS calculations were conducted using servers provided by ChemCompute (https://chemcompute.sonoma.edu/index.html), which is a website that allows students and researchers to easily run computational chemistry software for free. The input files were uploaded to the web via a user interface in the researcher mode on ChemCompute. Each job was run using 24 computer cores at a time, and went until the total energy converged to a global minimum or the allocated memory was exceeded. For files whose calculations exceeded the allocated memory, the Cartesian coordinates for the complex from the most recent iteration of the density function theory self consistent field calculation were turned into a new input file. By doing this, it was possible to append the progress of incomplete calculations together, thus allowing for some of larger complexes (i.e. the 1:3 complexes) to be completed. Once completed, the calculations were retrieved from ChemCompute, and analyzed using the program MacMolPlt (https://brettbode.github.io/wxmacmolplt/). MacMolPlt was used to visualize the chemical formations and interactions of the lowest stabilization energy for each complex. The energy for each trial was recorded with Microsoft excel, which was also used to do statistical analysis of the density functional theory results.

Statistical Analysis

Since there were no expected numbers for this experiment, no tests of significance were performed. Instead, the averaged (standard deviation was negligible) values pertaining to each acetylcholine-functional monomer complex were used in an equation to calculate the stabilization energy (ΔE) of that complex (Equation 1). The calculated total complex energy was substituted for the variable $E_{(template - monomer)}$. The calculated total energy for each template and monomer were substituted for $E_{(template)}$ and $E_{(monomer)}$ respectively. For a complex with more than one functional monomer in it, the total energy for the monomer was the sum of however many molecules of that monomer were in that complex. The resulting stabilization energy for each complex was then converted from atomic units (a.u.) to kilocalories/mole (kcal/mol), and then into kilojoules/mole (kJ/mol) (Equation 2).

Equation 1 - Calculation of Complex Stabilization Energy Using Calculated Total Complex and Molecular Energies

$$\Delta E = E_{(template - monomer)} - \{E_{(template)} + \sum E_{(monomer)}\}$$

Equation 2 – Conversion of Stabilization Energy from Atomic Units to Kilojoules per Mole

$$(\Delta E * 1\ a.u.). * \{(627.51\ kcal/mol) / (1\ a.u)\} * \{(4.184\ kJ/mol) / (1\ kcal/mol)\} = (\Delta E * 2625.50\ kJ/mol)$$

Results

Figure 1 – Conversion of Acetylcholinesterase Crystal Structure (PDB Code: 1EEA) into a Grid for Docking Study with AutoDock

a)

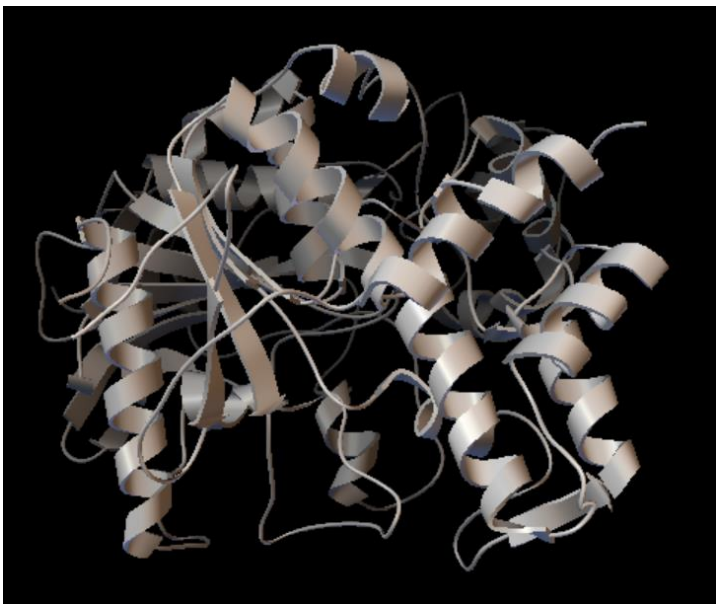

b)

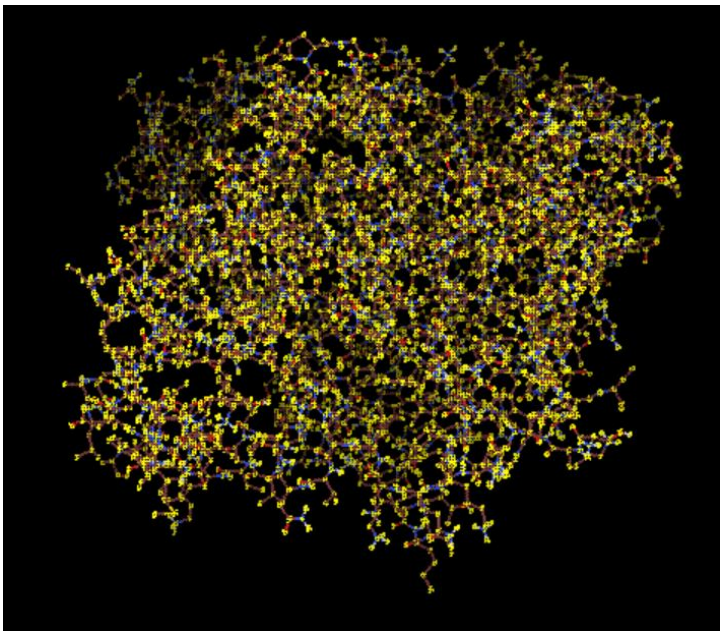

The crystal structure of an acetylcholinesterase isolated from *Electrophorus electricus* was downloaded from PDB (PDB code: 1EEA). This crystal structure was then used to perform a docking study with the software AutoDock, as shown in figure 1. The protein structure (a) was converted into a grid (b), with a grid point being made for every atom in the protein. The minimal spacing for every grid point was 0.375Å. The parameters for the ligand, acetylcholine, were then used to rank the top 10 sites where acetylcholine had the most favorable binding energy with acetylcholinesterase. The docking study was repeated 12 times to ensure the accuracy of the obtained results.

Figure 2 – A Visual Representation of AutoDock Analysis of Acetylcholine Interactions with Active Site Amino Acid Residues of Acetylcholinesterase

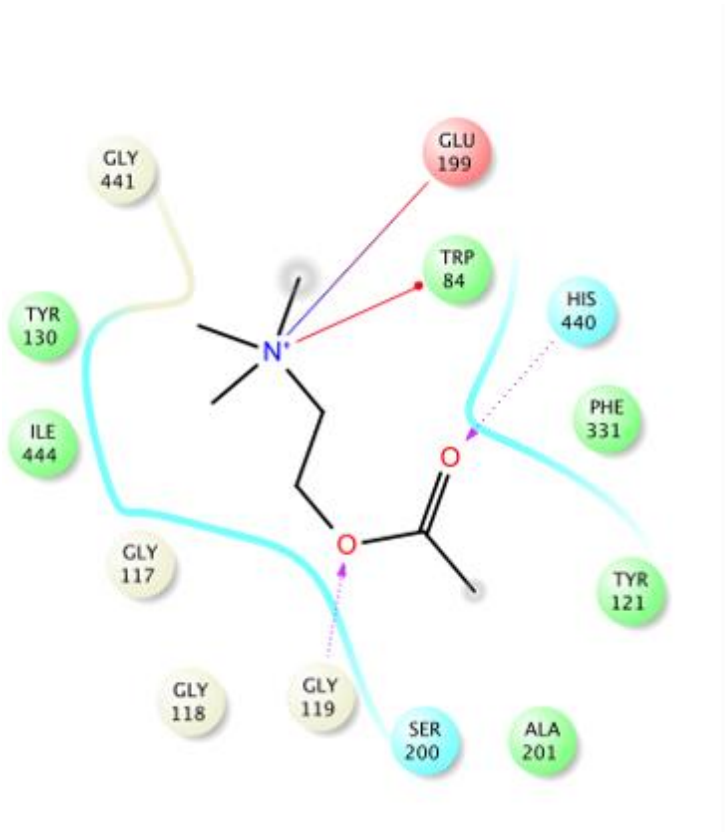

Figure 2 is a visual representation of the most favorable site for acetylcholine-acetylcholinesterase interaction, according to the docking study performed with AutoDock. This site was further analyzed using the visualization software called Maestro, which allowed for a clean representation of the site and the interactions that facilitate the ligand-protein interaction. The purple arrows extending from glycine 119 (Gly^{119}) and histidine (His^{440}) represent hydrogen bond interactions. The red line extending from tryptophan (Trp^{84}) represents a pi-cation interaction. Lastly, the red and blue line connecting glutamate (Glu^{199}) and acetylcholine represents an ionic interaction. Sussman et al. reported that His^{440} was a part of the active site of acetylcholinesterase, and that Gly^{119} was integral in guiding acetylcholine into said active site (Sussman, 1991).

Table 1 – AutoDock Results for Binding Energy of Acetylcholine Docked with Acetylcholinesterase Active Site Residues

Rank	Average Binding Energy (kJ/Mol)	Conformation (H-bonds)
1	**17.99±0.4**	**HIS440**
2	17.49±0.7	ARG349, ASP377
3	**-17.78±0.2**	**SER200, HIS440**
4	**-17.36±0.5**	**SER200**
5	**-17.03±0.3**	**GLY119, SER200, HIS440**
6	-16.19±0.6	PHE288, ARG289
7	-16.15±0.7	VAL71
8	-15.77±0.8	VAL71,GLN272
9	-16.02±0.2	ASP72
10	-15.65±0.4	0

Table 1 contains the top binding sites from the docking study of acetylcholine with acetylcholinesterase. The docking software, AutoDock, was used to compute the optimal sites for acetylcholine interaction with the protein. The software used a simplified forcefield in order to calculate the free binding energy of acetylcholine at each site. These calculations were facilitated by restricting the search space to sites where acetylcholine could fit and the flexibility of both the ligand and protein. Each site is listed in rank of favorability, along with their respective binding energies and any hydrogen bonding interactions they take part in. Notice interactions ranked 1, 3, 4, and 5 (bolded) all have the amino acid residues Ser^{200} and His^{440} involved, which were both reported by Sussman et al. to be involved in the active site of acetylcholinesterase. At the very least, these results further validated the Sussman group's assertion that acetylcholine interacted with Ser^{200} and $hist^{440}$ of acetylcholinesterase.

Figure 2 – Selection of Functional Monomer Library for GAMESS Analysis

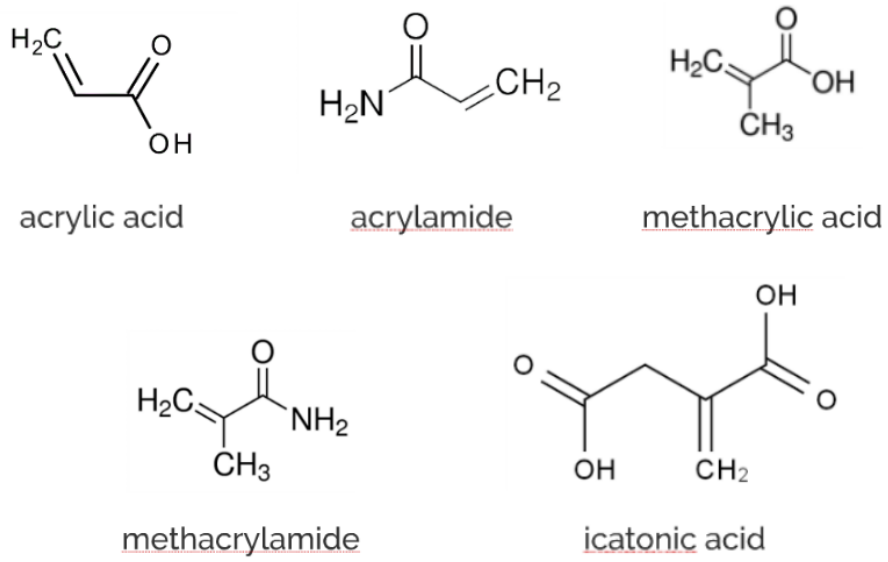

The chemical structures of the five functional monomers that were chosen for the experiment as displayed in figure 2. Chemicals were chosen based on the results of the docking study (figure 1 & table 1), which were cross-validated with the results of Sussman et al. Both Sussman et al. and the docking study we performed indicated that acetylcholine interactions with acetylcholinesterase were primarily hydrogen bonding, ionic, or due to dispersion forces. Of these three interactions, chemicals that could engage in hydrogen bonding or ionic interactions with acetylcholine were preferentially chosen. This decision was made because hydrogen bonding and ionic interactions are two of the strongest non-covalent biochemical interactions possible. These two interactions can also be easily facilitated by functional groups such as carboxylic acids or amides. Dispersion forces are also amongst the weakest of intramolecular forces, which require high electron density (i.e. phenyl groups) to become significant. Chemicals with such high electron density would be more computationally expensive to screen due to the nature of density functional theory. In addition, the selected chemicals have all been previously used to successfully synthesize MIPs (Algieri, 2014).

Table 2 - Density Functional Theory Results from GAMESS Analysis of Each Individual Molecule

Chemical name	Total Energy (a.u.)
Acetylcholine	-481.08
Methacrylic acid	-306.32
Acrylic acid	-267.03
Methacrylamide	-286.45
Acrylamide	-247.16
Itaconic acid	-494.81

The total energies returned by GAMESS for each individual compound are found in table 2. Each compound had its equilibrium geometry, otherwise called lowest total energy, calculated three times with the quantum calculator GAMESS (B3LYP, 6-31G(d,p), gas phase). GAMESS used the linear combination of basis set functions similar in mathematical form to Hartree-Fock orbitals in order to express the predicted electron density of a compound. The electron density for each compound was then used to calculate the total energy in terms of atomic units (a.u.). There was no significant standard deviation among the results for any of the compounds. These values were substituted into equation 1

($\Delta E = E_{(template\ -\ monomer)} - \{E_{(template)} + \sum E_{(monomer)}\}$) during the calculation of the stabilization energies for each complex. acetylcholine was substituted in for $E_{(template)}$. whereas functional monomers were substituted in for $E_{(monomer)}$ when calculating the stabilization energy for their associated complexes.

Table 3 – Results of Density Functional Theory Calculations for Acetylcholine-Methacrylic Acid Complexes

Complex	Trial 1 E (a.u.)	Trial 2 E (a.u.)	Trial 3 E (a.u.)	Average E (a.u.)
1 Acetylcholine : 1 Methacrylic Acid	-787.42	-787.42	-787.42	-787.42
1 Acetylcholine : 2 Methacrylic Acid	-1093.76	-1093.76	-1093.76	-1093.76
1 Acetylcholine : 3 Methacrylic Acid	-1400.11	-1400.11	-1400.11	-1400.11

Table 3 contains the raw data returned by the density functional theory calculations for each acetylcholine-methacrylic acid complex. Each complex had its equilibrium geometry, otherwise called lowest total energy, calculated three times with the quantum calculator GAMESS (B3LYP, 6-31G(d,p), gas phase). GAMESS used the linear combination of basis set functions similar in mathematical form to Hartree-Fock orbitals in order to express the predicted electron density of a complex. The electron density for each complex was then used to calculate the total energy in terms of atomic units (a.u.). The averaged values for each complex were substituted in for $E_{(template - monomer)}$ in equation 1 $(\Delta E = E_{(template\ -\ monomer)} - \{E_{(template)} + \sum E_{(monomer)}\})$.

Table 4 – Results of Density Functional Theory Calculations for Acetylcholine-Acrylic Acid Complexes

Complex	Trial 1 E (a.u.)	Trial 2 E (a.u.)	Trial 3 E (a.u.)	Average E (a.u.)
1 Acetylcholine : 1 Acrylic Acid	-748.141	-748.135	-748.1351	-748.137
1 Acetylcholine : 2 Acrylic Acid	-1015.18	-1015.18	-1015.183	-1015.183
1 Acetylcholine : 3 Acrylic Acid	-1282.23	-1282.23	-1282.232	-1282.232

Table 4 contains the raw data returned by the density functional theory calculations for each acetylcholine-acrylic acid complex. Each complex had its equilibrium geometry, otherwise called lowest total energy, calculated three times with the quantum calculator GAMESS (B3LYP, 6-31G(d,p), gas phase). GAMESS used the linear combination of basis set functions similar in mathematical form to Hartree-Fock orbitals in order to express the predicted electron density of a complex. The electron density for each complex was then used to calculate the total energy in terms of atomic units (a.u.). The averaged values for each complex were substituted in for $E_{(template - monomer)}$ in equation 1 $(\Delta E = E_{(template\ -\ monomer)} - \{E_{(template)} + \sum E_{(monomer)}\})$.

Table 5 – Results of Density Functional Theory Calculations for Acetylcholine-Methacrylamide Complexes

Complex	Trial 1 E (a.u.)	Trial 2 E (a.u.)	Trial 3 E (a.u.)	Average E (a.u.)
1 Acetylcholine : 1 Methacrylamide	-767.56	-767.56	-767.56	-767.56
1 Acetylcholine : 2 Methacrylamide	-1054.04	-1054.04	-1054.04	-1054.04
1 Acetylcholine : 3 Methacrylamide	-1340.50	-1340.50	-1340.50	-1340.50

Table 5 contains the raw data returned by the density functional theory calculations for each acetylcholine-methacrylamide acid complex. Each complex had its equilibrium geometry, otherwise called lowest total energy, calculated three times with the quantum calculator GAMESS (B3LYP, 6-31G(d,p), gas phase). GAMESS used the linear combination of basis set functions similar in mathematical form to Hartree-Fock orbitals in order to express the predicted electron density of a complex. The electron density for each complex was then used to calculate the total energy in terms of atomic units (a.u.). The averaged values for each complex were substituted in for $E_{(template - monomer)}$ in equation 1 $(\Delta E = E_{(template\ -\ monomer)} - \{E_{(template)} + \sum E_{(monomer)}\})$.

Table 6 - Results of Density Functional Theory Calculations for Acetylcholine-Acrylamide Complexes

Complex	Trial 1 E (a.u.)	Trial 2 E (a.u.)	Trial 3 E (a.u.)	Average E (a.u.)
1 Acetylcholine : 1 Acrylamide	-728.28	-728.28	-728.28	-728.28
1 Acetylcholine : 2 Acrylamide	-975.46	-975.46	-975.46	-975.46
1 Acetylcholine : 3 Acrylamide	-1222.64	-1222.63	-1222.63	-1222.63

Table 6 contains the raw data returned by the density functional theory calculations for each acetylcholine-acrylamide acid complex. Each complex had its equilibrium geometry, otherwise called lowest total energy, calculated three times with the quantum calculator GAMESS (B3LYP, 6-31G(d,p), gas phase). GAMESS used the linear combination of basis set functions similar in mathematical form to Hartree-Fock orbitals in order to express the predicted electron density of a complex. The electron density for each complex was then used to calculate the total energy in terms of atomic units (a.u.). The averaged values for each complex were substituted in for $E_{(template - monomer)}$ in equation 1 $(\Delta E = E_{(template\ -\ monomer)} - \{E_{(template)} + \sum E_{(monomer)}\})$.

Table 7 - Results of Density Functional Theory Calculations for Acetylcholine-Itaconic Acid Complexes

Complex	Trial 1 E (a.u.)	Trial 2 E (a.u.)	Trial 3 E (a.u.)	Average E (a.u.)
1 Acetylcholine : 1 Itaconic Acid	-975.92	-975.92	-975.92	-975.92
1 Acetylcholine : 2 Itaconic Acid	-1470.76	-1470.76	-1470.76	-1470.76
1 Acetylcholine : 3 Itaconic Acid	-1965.57	-1965.57	-1965.57	-1965.57

Table 7 contains the raw data returned by the density functional theory calculations for each acetylcholine-acrylamide acid complex. Each complex had its equilibrium geometry, otherwise called lowest total energy, calculated three times with the quantum calculator GAMESS (B3LYP, 6-31G(d,p), gas phase). GAMESS used the linear combination of basis set functions similar in mathematical form to Hartree-Fock orbitals in order to express the predicted electron density of a complex. The electron density for each complex was then used to calculate the total energy in terms of atomic units (a.u.). The averaged values for each complex were substituted in for $E_{(template - monomer)}$ in equation 1 $(\Delta E = E_{(template - monomer)} - \{E_{(template)} + \sum E_{(monomer)}\})$. Itaconic acid complexes had the lowest average total energies amongst all the complexes screened in this study (1ACh:1IA= -975.92 a.u., 1ACh:2IA= -1470.76 a.u., 1ACh:3IA= -1965.57 a.u.).

Table 8 – Calculated Stabilization Energies of acetylcholine-functional monomer Complexes Analyzed with GAMESS

Functional monomer (FM)	ΔE 1ACh:1FM (kJ/mol)	ΔE 1ACh:2FM (kJ/mol)	ΔE 1ACh:3FM (kJ/mol)
Methacrylic acid	-34.54	-101.82	-152.04
Acrylic acid	-76.34	-124	-177.17
Methacrylamide	-61.24	-130.82	-163.11
Acrylamide	-92.4	-150.77	-175.72
Itaconic Acid	-85.66	-180.44	-197.51

The stabilization energy for each complex that was screened is displayed in table 8. Each Functional monomer was placed into a complex with acetylcholine at a ratio of 1:1, 1:2, and 1:3. Density Functional Theory (B3LYP, 6-31G(d,p), gas phase) was then used in order to calculate the equilibrium geometry, or in other words the lowest total energy, for each complex. The stabilization energy for each complex was then calculated using the total energy of the complex and its respective compounds in equation 1 $\boldsymbol{(\Delta E = E_{(template\ -\ monomer)} - \{E_{(template)} + \sum E_{(monomer)}\})}$.

The calculated stabilization energy for each complex was then converted from atomic units (a.u.) to kilojoules per mole (kJ/mol) using equation 2 ***(ΔE * 1 a.u). * {(627.51 kcal/mol) / (1 a.u)} * {(4.184 kJ/mol) / (1 kcal/mol)} = (ΔE* 2625.50 kJ/mol)***.

Acetylcholine-itaconic acid (1ACh:X IA, where X= an integer value 1, 2, or 3) complexes had the lowest overall stabilization energy (ΔE 1 ACh:3 IA= -197.51kJ/mol), and the lowest stabilization energy among 1 acetylcholine:2 functional monomer complexes (ΔE 1ACh:2 IA= -180.44kJ/mol). Acrylamide formed the lowest stabilization energy among 1:1 complexes (ΔE 1ACh:1 A= -92.40 kJ/mol).

Figure 3 – A visual Representation of the 1 Acetylcholine:3 Itaconic Acid Complex with MacMolPlt

a)

b)

c)

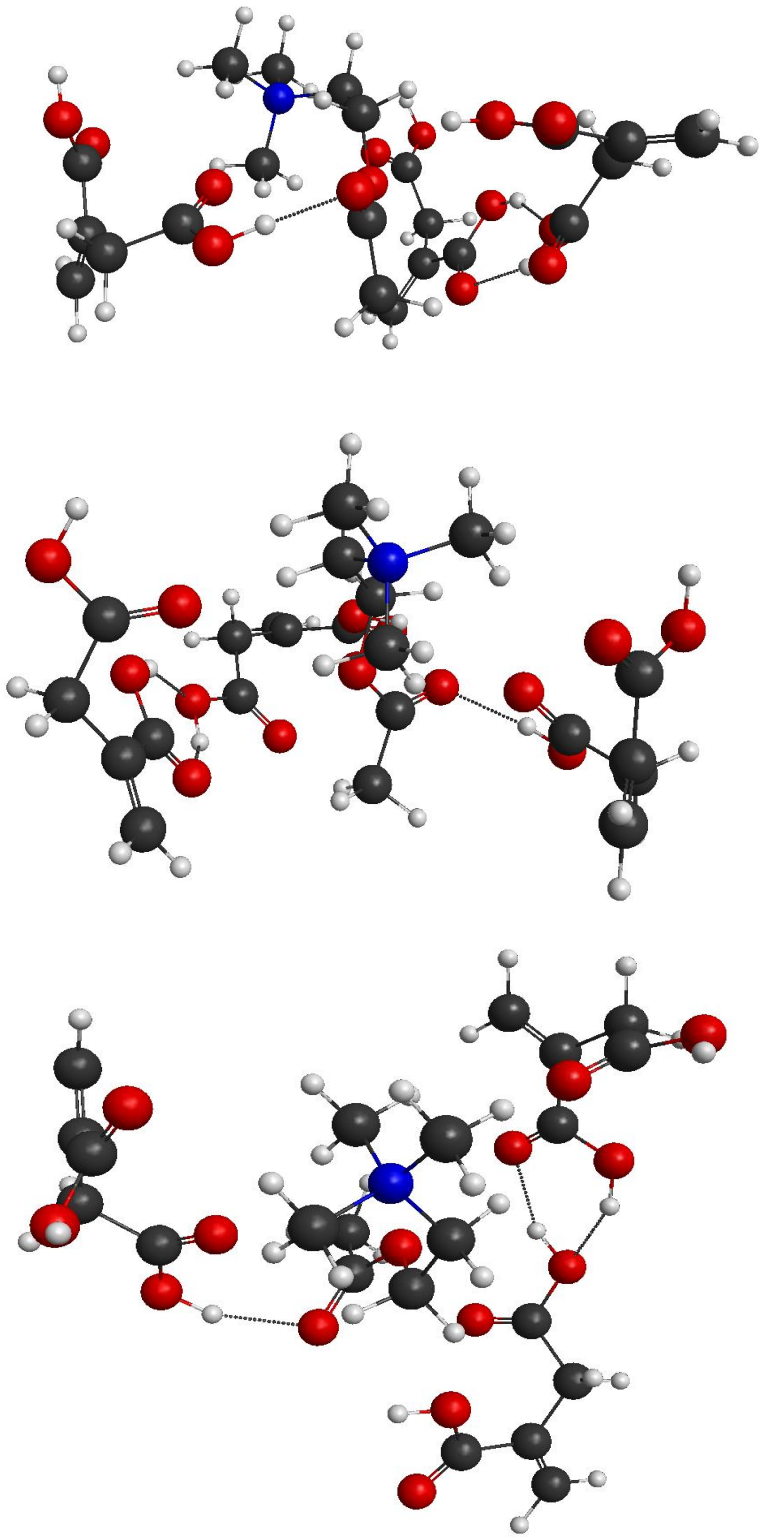

Figure 3 portrays the equilibrium geometry for the complex of 1 acetylcholine with 3 itaconic acids. Snapshots of complex in the predicted equilibrium geometry were rendered with the software Maestro. Maestro allowed for the visualization of the change in Cartesian coordinates as the equilibrium geometry was calculated by using the output file written by GAMESS. Both (a) and (b) show a sideways view of the complex from alternate angles, while in the equilibrium geometry. The third image (c) is a top-down view of the complex. Hydrogen bonding is denoted with dashed lines within each of the figures. Density functional theory predicted that this complex would be the most favorable among all the other complexes of 1 acetylcholine to 3 functional monomers (table 8). However, further studies are needed in order to validate this prediction.

Discussion

Biological instances of recognition sites for acetylcholine were studied first to learn what interactions are important for acetylcholine binding. This bio-mimetic approach is a tried and true method for creative innovation in the sciences. The results of Sussman et al. were used to validate the results of our docking study with the docking software AutoDock. We compared our results to their published findings, and found that there was a high degree of agreement between the two studies. In both of the studies, acetylcholine was found to interact with acetylcholinesterase via hydrogen bonding, ionic interactions, and dispersion forces (Figure 1). The pi-cation binding (seen between acetylcholine and Trp^{84} in figure 1) is a type of dispersion force, which is particularly generated by a large electron cloud. it was decided that an attempt to recapitulate this pi-cation interaction should not be made, due to the limited capability of density functional theory to model such high density systems. Instead, it was thought that GAMESS would have an easier time calculating the equilibrium geometry of smaller electron systems that did not feature large pi orbitals as seen in phenyl groups and other conjugated ring structures.

Therefore, five functional monomers were chosen for their functional groups that could participate in either hydrogen bonding (seen between acetylcholine and both Gly^{119} and His^{440} in figure 1) or ionic interactions (seen between acetylcholine and Glu^{199} in figure 1). Of the three different interactions involved in acetylcholine-acetylcholinesterase interaction, we chose functional monomers that can participate in hydrogen bonding and ionic interactions because they are among the strongest non-covalent biochemical interactions possible. In addition, all of the functional monomers selected have been used previously in the successful synthesis of MIP (Algieri, 2014). The crystal structures for these functional monomers, and acetylcholine, were retrieved from online sources. This is important as the lattice constants retrieved with the crystal

structures were used to create a unit cell of proper size, in which the system was then analyzed. These measures assured that the scale, bond lengths and degrees of rotation for the representation of each molecule in Avogadro (the molecular editing program used to prepare the input Cartesian coordinates of the screened complexes) were accurate from the start of the density functional theory calculations.

Density functional theory was chosen because it is an exceedingly popular computational method among experts in the synthesis of MIPs. The density functional theory calculations were done using the B3LYP correlational functional, which is generally preferred by many groups for providing accurate results at a relatively low computational cost (Young, 2001). In addition, the polarization 6-31G(d,p) basis set that was used in the calculations allows for the accurate linear combination of atomic orbitals up to the d and p orbitals at a moderate computational cost. Due to prepare the analyzed complexes, it is reasonable to have a good amount of faith in the total complex energy results obtained from the density functional theory calculations. Therefore, it is theorized that itaconic acid (Table 8; ΔE 1 ACh:3 IA= -197.51kJ/mol & ΔE 1 ACh:2 IA= -180.44kJ/mol) will form the optimal acetylcholine MIP.

MIPs synthesized using acrylamide will serve to check the density functional theory results, since it had the most favorable 1 acetylcholine: 1 functional monomer complex (ΔE 1 ACh:1 A= -92.40 kJ/mol) as well as the second most favorable 1 acetylcholine: 2 functional monomer and 1 acetylcholine: 3 functional monomer complexes (ΔE 1 ACh:2 IA= -150.75kJ/mol & ΔE 1 ACh:3 IA= -175.72kJ/mol). This will not only provide a way to compare the functionality of two MIP made with different functional monomers, but will also allow for validation of the computational approach utilized in this study. If MIPs made with itaconic acid are proven to be

more efficient than MIPs made with acrylamide, then this study will set a precedent that free software can be used to rationally design a MIP with recognition for a template element.

Despite the confidence in the results obtained through density functional theory, it is interesting to note that itaconic acid actually had the lowest total energy for 1:1, 1:2, and 1:3 acetylcholine-functional monomer complexes (Table 7). However, when those values were used to calculate the stabilization energy for each complex, itaconic acid lost the lowest energy among 1 acetylcholine: 1 functional monomer complexes to the acetylcholine-acrylamide complex. In general, the decrease seen in complex energy as the ratio of functional monomer to acetylcholine increased was greater than the free energy calculated for every single molecule (table 2). This means that there was a synergistic effect that made complexation more favorable as the ratio of functional monomer to acetylcholine was increased. Perhaps itaconic lost the most favorable 1:1 complex to acrylamide because the observed synergistic effect only applied to complexes with a ratio of 1 acetylcholine to 2 functional monomers or more. Therefore, acrylamide probably overtook itaconic for the most favorable stabilization energy because it formed a more stable complex in a 1:1 ratio. However, as the ratio of functional monomers to acetylcholine was increased, the synergistic effect on stabilization energy made itaconic acid complex more favorable. Although there is still a high degree of confidence in this study's results, this small discrepancy in lowest total energies and lowest stabilization energies could also be an early indication that there is some inaccuracy in the density functional results.

Acetylcholine-functional monomer complexes were only investigated up to a ratio of 1:3 because larger ratios give way to unwanted functional monomer-functional monomer interactions. Such interactions could have confounded the results of the density functional theory by artificially lowering the stabilization energy of a complex. However, since the interaction between

acetylcholine and these functional monomer complexes was modeled with the use of approximations, it is still possible that the exact way in which functional monomers interact with acetylcholine will be different than predicted. For example, the lowest equilibrium geometry predicted by GAMESS may not be the lowest equilibrium geometry in reality. Additionally, adding the solvent and cross-linking agent into the mix may affect the interactions responsible for making the acetylcholine-functional monomer complex pre-polymerization. These factors could potentially negate the findings of this study in a worst case scenario. However, this possibility only strengthens the need to make acetylcholine MIPs with acrylamide as well as itaconic acid. It may also be necessary to make MIPs with another functional monomer in order to further validate the results of this study.

This thinking is why it was so important to model as many suitable functional monomers as possible, since there are many confounding factors that can potentially affect the viability of a functional monomer (Wilson, 2005). These confounding factors include the other chemicals used in the synthesis of MIPs (i.e. crosslinking agents, solvent, impurities), the denaturation that comes from repeated rebinding (Rosengren, 2009), and other important metrics besides the stabilization energy of the pre-polymerization acetylcholine-functional monomer complex. Other important metrics for the synthesis of MIPs that have been noted to cause complications in recent years include vibrational frequency (Prasad and Rai, 2012), dielectric constants (Rosengren, 2009), and the Snyder polarity index (Rosengren, 2009). Therefore, the more suitable monomers that get identified the better prepared we will be to surpass any obstacles that may arise.

If these results are proven to be accurate, then it will be a boon to the growing field of computational chemistry. This would set an example of density functional theory being used, with free software and donated server time, to rationally design a molecularly imprinted polymer.

Molecularly imprinted polymers have already seen an explosion of applications in medical biosensors, chromatographic purposes, and a many others. Therefore, validating the approach used in this study would set a precedent for other groups, with limited resources and time, to rationally design MIPs for a molecule somewhat similar in size to acetylcholine. We predict that we will be able to synthesize a hydrogel derived acetylcholine MIP, where the experimental conditions can be modulated to yield either a thin layer or block of material.

The specific applications of an acetylcholine MIP with high selectivity and affinity range from physiological research, filters in industry, and biomedical devices in medicine. For instance, acetylcholine analogs are frequently used as pesticides, and run-off into public waters of these chemicals are a growing concern. An acetylcholine MIP could potentially be used to filter out these pesticides, or serve as a biosensor to detect and signal their presence in water samples. Similarly, an acetylcholine MIP could be utilized in a biosensor to test for the physiological release of acetylcholine at the site of amputation in patients during phantom motor control. Studies have already shown that amputees can control phantom limbs of lost appendages naturally (De Graaf, 2016). Furthermore, this phantom motor control can elicit electromyographic (EMG) signals at the site of amputation (Imaizumi, 2014). These EMG recordings are indicative of muscular depolarization, usually triggered by acetylcholine transmission. However, no study has confirmed the continued transmission of acetylcholine at the site of amputation. Therefore, an acetylcholine MIP could be used to investigate this questions. If acetylcholine transmission was preserved, and could be adequately mapped to intended movement, then an acetylcholine MIP could be utilized in a biosensor to control prosthetic devices in a more natural manner. This manner could even improve upon spatial and temporal limitations in terms of resolution for current prostheses control paradigms.

Acknowledgements

Thank you to Professor Mark Perri of Sonoma State University for providing an ample allocation of server time to conduct the GAMESS calculations for this study. The advice and guidance of professors Church, Palandage, Perri, and Thilakarathne were critically important in completing this study.

References

Alexander, C., Andersson, H. S., Andersson, L. I., Ansell, R. J., Kirsch, N., Nicholls, I. A., … Whitcombe, M. J. (2006). Molecular imprinting science and technology: a survey of the literature for the years up to and including 2003. *Journal of Molecular Recognition*, *19*(2), 106–180. https://doi.org/10.1002/jmr.760

Algieri, C., Drioli, E., Guzzo, L., & Donato, L. (2014). Bio-Mimetic Sensors Based on Molecularly Imprinted Membranes. *Sensors*, *14*(8), 13863–13912. https://doi.org/10.3390/s140813863

Ahmadi, F., Ahmadi, J., & Rahimi-Nasrabadi, M. (2011). Computational approaches to design a molecular imprinted polymer for high selective extraction of 3,4-methylenedioxymethamphetamine from plasma. *Journal of Chromatography A*, *1218*(43), 7739–7747. https://doi.org/10.1016/j.chroma.2011.08.020

Askarinejad, S., & Rahbar, N. (2015). Toughening mechanisms in bioinspired multilayered materials. *Journal of The Royal Society Interface*, *12*(102), 20140855. https://doi.org/10.1098/rsif.2014.0855

Asman, S., Mohamad, S., & Sarih, N. M. (2015). Exploiting β-Cyclodextrin in Molecular Imprinting for Achieving Recognition of Benzylparaben in Aqueous Media. *International Journal of Molecular Sciences*, *16*(2), 3656–3676. https://doi.org/10.3390/ijms16023656

Barros, L. A. de, Pereira, L. A., Custódio, R., & Rath, S. (2014). A novel computational approach for development of highly selective fenitrothion imprinted polymer: theoretical predictions and experimental validations. *Journal of the Brazilian Chemical Society*, *25*(4), 619–628. https://doi.org/10.5935/0103-5053.20140009

Bayat, M., Hassanzadeh-Khayyat, M., & Mohajeri, S. A. (2014). Determination of Diazinon Pesticide Residue in Tomato Fruit and Tomato Paste by Molecularly Imprinted Solid-Phase Extraction Coupled with Liquid Chromatography Analysis. *Food Analytical Methods*, *8*(4), 1034–1041. https://doi.org/10.1007/s12161-014-9984-6

Chen, Y.-P., Liu, B., Lian, H.-T., & Sun, X.-Y. (2011). Preparation and Application of Urea Electrochemical Sensor Based on Chitosan Molecularly Imprinted Films. *Electroanalysis*, *23*(6), 1454–1461. https://doi.org/10.1002/elan.201000693

Crouch, R. D. (1997). A Laboratory Book of Computational Organic Chemistry (Hehre, Warren J.; Shusterman, Alan J.; Huang, W. Wayne). *Journal of Chemical Education*, *74*(6), 628. https://doi.org/10.1021/ed074p628

De Graaf, J. B. et al. "Phantom Hand and Wrist Movements in Upper Limb Amputees Are Slow but Naturally Controlled Movements." *Neuroscience* 312 (2016): 48–57. *ScienceDirect*. Web.

De Luca, G., Donato, L., García Del Blanco, S., Tasselli, F., & Drioli, E. (2011). On the Cause of Controlling Affinity to Small Molecules of Imprinted Polymeric Membranes Prepared by Noncovalent Approach: A Computational and Experimental Investigation. *The Journal of Physical Chemistry B*, *115*(30), 9345–9351. https://doi.org/10.1021/jp2006638

Diñeiro, Y., Menéndez, M. I., Blanco-López, M. C., Lobo-Castañón, M. J., Miranda-Ordieres, A. J., & Tuñón-Blanco, P. (2006). Computational predictions and experimental affinity distributions for a homovanillic acid molecularly imprinted polymer. *Biosensors and Bioelectronics*, *22*(3), 364–371. https://doi.org/10.1016/j.bios.2006.03.027

Guan, Huanan et al. "The Novel Acetylcholinesterase Biosensors Based on Liposome Bioreactors–chitosan Nanocomposite Film for Detection of Organophosphates Pesticides." *Food Research International* 49.1 (2012): 15–21. *ScienceDirect*. Web.

Hadizadeh, F., Hassanpour Moghadam, M., & Mohajeri, S. A. (2013). Application of molecularly imprinted hydrogel for the preparation of lactose-free milk. *Journal of the Science of Food and Agriculture*, *93*(2), 304–309. https://doi.org/10.1002/jsfa.5757

Hawkes, E. W., Eason, E. V., Christensen, D. L., & Cutkosky, M. R. (2015). Human climbing with efficiently scaled gecko-inspired dry adhesives. *Journal of The Royal Society Interface*, *12*(102), 20140675. https://doi.org/10.1098/rsif.2014.0675

Imaizumi, Shu et al. "Agency over a Phantom Limb and Electromyographic Activity on the Stump Depend on Visuomotor Synchrony: A Case Study." *Frontiers in Human Neuroscience* 8 (2014): 545. *Frontiers*. Web.

Jimenez-Solomon, M. F., Song, Q., Jelfs, K. E., Munoz-Ibanez, M., & Livingston, A. G. (2016). Polymer nanofilms with enhanced microporosity by interfacial polymerization. *Nature Materials, advance online publication*. https://doi.org/10.1038/nmat4638

Khairi, N. A. S., Yusof, N. A., Abdullah, A. H., & Mohammad, F. (2015). Removal of Toxic Mercury from Petroleum Oil by Newly Synthesized Molecularly-Imprinted Polymer. *International Journal of Molecular Sciences*, *16*(5), 10562–10577. https://doi.org/10.3390/ijms160510562

Lattach, Y., Archirel, P., & Remita, S. (2012). Influence of the chemical functionalities of a molecularly imprinted conducting polymer on its sensing properties: electrochemical measurements and semiempirical DFT calculations. *The Journal of Physical Chemistry. B*, *116*(5), 1467–1481. https://doi.org/10.1021/jp2071524

Liu, M., Pi, J., Wang, X., Huang, R., Du, Y., Yu, X., … Shea, K. J. (2016). A sol-gel derived pH-responsive bovine serum albumin molecularly imprinted poly(ionic liquids) on the surface of multiwall carbon nanotubes. *Analytica Chimica Acta*, *932*, 29–40. https://doi.org/10.1016/j.aca.2016.05.020

Nakamura, Hideaki, and Isao Karube. "Current Research Activity in Biosensors." *Analytical and Bioanalytical Chemistry* 377.3 (2003): 446–468. *link.springer.com*. Web.

Nicholls, I. A., Andersson, H. S., Golker, K., Henschel, H., Karlsson, B. C. G., Olsson, G. D., … Wikman, S. (2011). Rational design of biomimetic molecularly imprinted materials: theoretical and computational strategies for guiding nanoscale structured polymer development. *Analytical and Bioanalytical Chemistry*, *400*(6), 1771–1786. https://doi.org/10.1007/s00216-011-4935-1

Piletska, E. V., Romero-Guerra, M., Guerreiro, A. R., Karim, K., Turner, A. P. F., & Piletsky, S. A. (2005). Adaptation of the molecular imprinted polymers towards polar environment. *Analytica Chimica Acta*, *542*(1), 47–51. https://doi.org/10.1016/j.aca.2005.01.034

Prasad, B. B., & Rai, G. (2012). Study on monomer suitability toward the template in molecularly imprinted polymer: an ab initio approach. *Spectrochimica Acta. Part A, Molecular and Biomolecular Spectroscopy*, *88*, 82–89. https://doi.org/10.1016/j.saa.2011.11.061

Puoci, F., Iemma, F., Cirillo, G., Picci, N., Matricardi, P., & Alhaique, F. (2007). Molecularly Imprinted Polymers for 5-Fluorouracil Release in Biological Fluids. *Molecules*, *12*(4), 805–814. https://doi.org/10.3390/12040805

Rosengren, A. M., Golker, K., Karlsson, J. G., & Nicholls, I. A. (2009). Dielectric constants are not enough: Principal component analysis of the influence of solvent properties on molecularly imprinted polymer–ligand rebinding. *Biosensors and Bioelectronics*, *25*(3), 553–557. https://doi.org/10.1016/j.bios.2009.06.042

Saridakis, E., Khurshid, S., Govada, L., Phan, Q., Hawkins, D., Crichlow, G. V., … Chayen, N. E. (2011). Protein crystallization facilitated by molecularly imprinted polymers- Supplemental Information. *Proceedings of the National Academy of Sciences*, *108*(27), 11081–11086. https://doi.org/10.1073/pnas.1016539108

Simon, Daniel T. et al. "An Organic Electronic Biomimetic Neuron Enables Auto-Regulated Neuromodulation." *Biosensors and Bioelectronics* 71 (2015): 359–364. *ScienceDirect*. Web.

Suedee, R., Seechamnanturakit, V., Suksuwan, A., & Canyuk, B. (2008). Recognition Properties and Competitive Assays of a Dual Dopamine/Serotonin Selective Molecularly Imprinted Polymer. *International Journal of Molecular Sciences*, *9*(12), 2333–2356. https://doi.org/10.3390/ijms9122333

Sun, H., Qiao, F., & Liu, G. (2006). Characteristic of theophylline imprinted monolithic column and its application for determination of xanthine derivatives caffeine and theophylline in green tea. *Journal of Chromatography. A*, *1134*(1–2), 194–200. https://doi.org/10.1016/j.chroma.2006.09.004

Suntornnond, R., An, J., Tijore, A., Leong, K. F., Chua, C. K., & Tan, L. P. (2016). A Solvent-Free Surface Suspension Melt Technique for Making Biodegradable PCL Membrane Scaffolds for Tissue Engineering Applications. *Molecules*, *21*(3), 386. https://doi.org/10.3390/molecules21030386

Sussman, J. L., Harel, M., Frolow, F., Oefner, C., Goldman, A., Toker, L., & Silman, I. (1991). Atomic structure of acetylcholinesterase from Torpedo californica: a prototypic acetylcholine-binding protein. *Science*, *253*(5022), 872–879. https://doi.org/10.1126/science.1678899

Wach, A., Chen, J., Falls, Z., Lonie, D., Mojica, E.-R., Aga, D., … Zurek, E. (2013). Determination of the Structures of Molecularly Imprinted Polymers and Xerogels Using an Automated Stochastic Approach. *Analytical Chemistry*, *85*(18), 8577–8584. https://doi.org/10.1021/ac402004z

Wei, Shuting, Michael Jakusch, and Boris Mizaikoff. "Capturing Molecules with Templated materials—Analysis and Rational Design of Molecularly Imprinted Polymers." *Analytica Chimica Acta* 578.1 (2006): 50–58. *CrossRef*. Web.

Wei, S., Jakusch, M., & Mizaikoff, B. (2007). Investigating the mechanisms of 17β-estradiol imprinting by computational prediction and spectroscopic analysis. *Analytical and Bioanalytical Chemistry*, *389*(2), 423–431. https://doi.org/10.1007/s00216-007-1358-0

Wilson, George S., and Raeann Gifford. "Biosensors for Real-Time in Vivo Measurements." *Biosensors and Bioelectronics* 20.12 (2005): 2388–2403. *ScienceDirect*. Web. 20th Anniversary of Biosensors and Bioelectronics20th Anniversary of Biosensors and Bioelectronics.

Yañez, F., Chianella, I., Piletsky, S. A., Concheiro, A., & Alvarez-Lorenzo, C. (2010). Computational modeling and molecular imprinting for the development of acrylic polymers with high affinity for bile salts. *Analytica Chimica Acta*, *659*(1–2), 178–185. https://doi.org/10.1016/j.aca.2009.11.054

Young, D. C. (2001). Density Functional Theory. In *Computational Chemistry* (pp. 42–48). John Wiley & Sons, Inc. Retrieved from http://onlinelibrary.wiley.com/doi/10.1002/0471220655.ch5/summary